Redox Biology 36 (2020) 101596

Contents lists available at ScienceDirect

Redox Biology

journal homepage: www.elsevier.com/locate/redox

Obesity promotes gastric cancer metastasis via diacylglycerol acyltransferase 2-dependent lipid droplets accumulation and redox homeostasis

Shuai Li[a,**,1], Teng Wu[a,1], Yun-Xin Lu[b,1], Jin-Xiang Wang[a], Feng-Hai Yu[a], Mei-Zhu Yang[c], Yi-Jia Huang[c], Zhi-Jing Li[c], Sen-Lan Wang[d], Ling Huang[d], Lei Lu[a], Tian Tian[b,*]

[a] Department of Biochemistry and Molecular Biology, GMU-GIBH Joint School of Life Sciences, Guangzhou Medical University, Guangzhou, 511436, PR China
[b] Sun Yat-sen University Cancer Center, State Key Laboratory of Oncology in South China, Collaborative Innovation Center for Cancer Medicine, Guangzhou, 510060, PR China
[c] Department of Clinical Medicine, The Third Clinical School of Guangzhou Medical University, Guangzhou, 511436, PR China
[d] The Third Affiliated Hospital of Guangzhou Medical University, Guangzhou, 510510, PR China

ARTICLE INFO

Keywords:
DGAT2
Gastric cancer
Lipid droplets
Anoikis resistance
NADPH

ABSTRACT

Experimental and molecular epidemiological studies indicate important roles for adipose tissue or high-fat diet (HFD) in tumor growth and metastasis. Gastric cancer (GC) possesses a metastatic predilection for the adipocyte-rich peritoneum. However, the precise molecular relevance of HFD in the peritoneal metastasis of GC remains unclear. Here, we showed that HFD causes obvious fat accumulation and promotes peritoneal dissemination of GC *in vivo*. Peritoneum-derived adipocytes induces robust lipid droplet (LD) accumulation and fatty acid oxidation in GC cells through transcriptional upregulation of DGAT2 in a C/EBPα-dependent manner and prevents anoikis during peritoneal dissemination. Treatment of GC cells with FAs or coculture with adipocytes induces intracellular formation of LDs and production of NADPH to overcome oxidative stress *in vitro*. Importantly, overexpression of DGAT2 was identified as an independent predictor of poor survival that promotes lung and peritoneal metastasis of GC, and genetic or pharmacological inhibition of DGAT2, via disruption of lipid droplet formation in a lipid-rich environment, enhances the sensitivity of GC to anoikis *in vitro* and inhibits peritoneal metastasis *in vivo*. Overall, our findings highlight the notion that DGAT2 may be a promising therapeutic target in GC with peritoneal implantation and provide some evidence for uncovering the link between obesity and tumor metastasis.

1. Introduction

Gastric cancer (GC) ranks fourth in incidence and second in cancer-related death worldwide [1]. Obesity is a major global health challenge and was reinforced as a well-established risk factor for human cancers, including GC, by a recent summary conducted by the International Agency for Research on Cancer and previous epidemiological studies [2,3]. As the second leading preventable cause of cancer [4], crosstalk between obesity and cancer warrants further investigation.

Metastasis to the omentum or peritoneum was observed in more than half of advanced GC cases and contributes to a five-year overall survival of less than 7% [5]. However, the underlying molecular mechanisms of this metastatic predilection have not been clearly elucidated, and therapeutic strategies are lacking. Resistance to anoikis, a kind of intrinsic apoptosis initiated by detachment from the extracellular matrix (ECM) and characterized by decreased absorption of glucose and increased production of reactive oxygen species (ROS), is a key step during tumor metastasis. As the major intracellular redox equivalent, growing evidence has demonstrated key roles of nicotinamide adenine dinucleotide phosphate (NADPH) homeostasis in anoikis resistance and tumor metastasis or chemoresistance [6–8].

Rapidly proliferating tumor cells generally require high amounts of cholesterol for synthesis of membranous organelles and fatty acids (FAs), as FA oxidation (FAO) can produce large amounts of intermediates, including NADPH, to meet the demand of energy supply and ROS detoxification [9–12]. Thus, targeting key enzymes mediating fatty

* Corresponding author. Sun Yat-sen University Cancer Center, 651 Dongfeng East Road, Guangzhou, 510060, PR China.
** Corresponding author. Guangzhou Medical University, Guangzhou, 511436, PR China.
E-mail addresses: gundam-speed@163.com (S. Li), tiantian@sysucc.org.cn (T. Tian).
[1] S. Li, T. Wu and Y.-X. Lu contributed equally to this work.

https://doi.org/10.1016/j.redox.2020.101596
Received 26 February 2020; Received in revised form 10 May 2020; Accepted 23 May 2020
Available online 29 May 2020

acid metabolism, such as CD36 and CPT1A [11,13], has been proven effective in suppressing cancer metastasis. Recent studies have also demonstrated that adipocytes can promote metastasis in a wide range of tumors, including breast cancer [14,15], ovarian cancer [16,17], melanoma [18], and gastric cancer [19].

Exogenous FAs need to be re-esterified to diacylglycerol to form triglycerides (TGs) before oxidation for NADPH synthesis. Key enzymes responsible for TG synthesis include acyl CoA: diacylglycerol acyltransferase (DGAT) enzymes, DGAT1 and DGAT2 [20,21]. Both DGAT enzymes, though evolutionarily unrelated, catalyze the same reaction, utilizing diacylglycerol and fatty acyl CoAs as substrates to form TGs [20,21]. DGAT1 is localized exclusively to the endoplasmic reticulum and has a broader substrate specificity (with respect to acyl acceptors) than DGAT2 [20,22–25]. In contrast, DGAT2 is found both in the endoplasmic reticulum and around lipid droplets (LDs) and appears to be the major enzyme contributing to TG synthesis [22,23,25,26], as mice lacking the enzyme have a more than a 90% reduction in TGs and die shortly after birth [26].

In this study, our findings uncover that DGAT2-catalyzed TG synthesis plays critical roles in protecting cells from lipid-rich environments and provide preclinical clues for applying DGAT2 as a therapeutic target in metastasis treatment.

2. Materials and methods

2.1. Human tissue samples

GC tissue specimens (N = 318) were collected from patients who underwent surgical resection at the Sun Yat-sen University Cancer Center (SYSUCC, Guangzhou, China) after obtaining written informed consent and in accordance with our Institutional Review Board and the Declaration of Helsinki (Supplementary Table 1). Eight freshly collected primary tumor tissues and matched metastasis tissues were frozen and stored in liquid nitrogen until needed for protein extraction.

2.2. Adipocyte separation and purification

Adipocytes were extracted from omental tissue specimens obtained from patients underwent surgical procedures at Sun Yat-sen University Cancer Center according to a previous report [11]. Each subject provided informed consent, and the study protocol was approved by the Hospital Ethics Review Board. Briefly, approximately 400–600 mg of adipose tissue was washed several times in D-Hank's buffer, minced finely using surgical scissors and incubated in 0.2% collagenase type I (Sigma-Aldrich, Saint Louis, USA) digestion buffer at 37 ˚C with constant agitation for approximately 30 min. Once digested, the liquid was separated into three layers: the upper, intermediate and bottom layer contained yellow oily lipocytes, adipose tissue and mononuclear cells in buffer, respectively. The buffer from the bottom layer was then carefully collected and centrifuged at 1500 rpm for 10 min in a microtube containing DMEM/F12 with 10% fetal bovine serum. The above steps were repeated 2–3 times until all adipose tissue was completely digested. Cell pellets were then suspended in medium (DMEM/F12 + 10% FBS) and immediately utilized for coculture with GC cells.

2.3. Immunohistochemistry and immunoblotting analysis

Immunohistochemical and immunoblotting analyses were conducted according to standard procedures as described previously [27]. DAB substrate was used to detect protein expression, and counterstaining was carried out using hematoxylin. The levels of DGAT2 immunostaining were evaluated independently by two pathologists who were blinded to the survival outcomes of the participants, based on both the proportion of positively stained tumor cells (1, < 25%; 2, 25%–50%; 3, 50%–75%; 4, 75%–100%) and the intensity of staining (negative, 0; weak, 1; moderate, 2; strong, 3). The immunostaining results were calculated by multiplying the stain intensity by the stain area (staining index, SI) as previously described [28]. The IHC staining index score of ≥6 was used to define tumors with high DGAT2 expression and a staining index score of ≤4 was used to indicate low DGAT2 expression. The antibodies used in our study were as follows: DGAT2 (ABclonal, #A13891, 1:1000 for WB; 1:200 for IHC), C/EBPα (CST, #8178, 1:1000 for WB; 1:200 for IHC) and GAPDH (Proteintech, #60004-1-lg, 1:5000 for WB).

2.4. Lentiviral or siRNA transduction

To knockdown the expression of DGAT2, lentivirus containing short hairpin RNA (shRNA) targeting DGAT2 or a nontarget oligonucleotide was synthesized by GenePharma (Suzhou, China). The shRNA target sequences were 5′-gctgaccaccaggaactatat-3′ (#1) and 5′-gcactgattgctggctcatcg-3′ (#2). Stable cell lines were selected with 5 μg/mL puromycin (Sigma-Aldrich, USA), and knockdown efficiency was confirmed by immunoblotting assays. For siRNA knockdown, C/EBPα siRNA and a control siRNA were purchased from RiboBio (Guangzhou, China). The siRNA target sequences were 5′-ggcaactctagtatttaggataa-3’ (#1) and 5′-accaccattttatttggtttttg-3’ (#2).

2.5. ROS, NADPH/NADP+, GSH/GSSG detection

ROS levels were determined as described previously [6,29]. Briefly, cells were incubated with 10 μM DCF-DA or 5 μM Mito-SOX at 37 ˚C for 30 min. Then, the cells were collected and resuspended in PBS. Fluorescence was immediately measured using a flow cytometer (Beckman, CytoFLEX). Intracellular levels of NADPH/NADP+ and GSH/GSSG were measured using the NADP/NADPH-Glo kit (Promega, #G9081, Wisconsin, USA) or GSH/GSSG-Glo kit (Promega, #V6612, Wisconsin, USA) according to the manufacturer's instructions.

2.6. Lipid staining assay

Oil Red O was used for neutral lipid staining. Briefly, cells were washed with PBS and incubated with 0.5% Oil Red O (Sigma-Aldrich) solution for 10 min at room temperature. Cell nuclei were counterstained with 2 μg/mL DAPI (BioFroxx, #1155MG010) or hematoxylin, and visualized under a fluorescence microscope. For confocal analysis, cells were fixed for 15 min in 4% formaldehyde/PBS, washed with 0.2% Triton-X 100/PBS and incubated with BODIPY 493/503 (Thermo Fisher Scientific, D3922) and DAPI for 30 min and 5 min at room temperature, respectively.

2.7. Animal experiments

Female BALB/c nude mice (3–4 weeks old) and SCID mice were obtained from the Laboratory Animal Center of Guangdong Province (Guangzhou, China). For the lung metastasis model, DGAT2 knockdown and control GC cells (2×10^6) resuspended in 200 μL of PBS were injected into the tail veins of nude mice (5 mice/group). Mice were sacrificed with cervical dislocation, and the lungs were removed and embedded in paraffin to histopathologically examine the metastatic locus as described previously [30]. Peritoneal dissemination was evaluated through intraperitoneal injection. In brief, DGAT2 knockdown and control GC cells (3×10^6) in 400 μL of PBS were injected into the peritoneal cavity. Peritoneum metastasis (nude or SCID mice, 6 mice/group) was examined and recorded when mice were killed at 30 days after injection. For survival analysis, survival (10 nude mice/group) time was recorded. A high-fat diet (Western diet) was purchased from Dyets (HFHC), and nude mice and SCID mice were given either a low-fat (LFD) or a high-fat (HFD) diet for 2–3 months before GC cells were injected. All animal procedures were in accordance with the guidelines of the Institutional Animal Care and Use Committee and the guidelines of the Guangzhou Medical University and Sun Yat-sen University

Cancer Center.

2.8. Statistical analyses

For comparison of the significant differences between two groups, Student's *t*-test was used. Matched groups (three or more) were compared using one-way analysis of variance [31] and Tukey's multiple comparisons test. For correlation analysis between two continuous variables, *P* values were calculated by Pearson's correlation test. Survival curves were plotted using the Kaplan-Meier method and compared by log-rank test. The parameters with *P* less than 0.05 in univariate analyses were included in the multivariable Cox analysis. Statistical analyses were performed with GraphPad version 6.0 or SPSS 20.0. A *P* less than 0.05 was considered statistically significant, and all statistical tests were two-sided.

The details for cell lines and reagents, RNA extraction and qPCR analysis, Apoptosis analysis, anoikis assay, soft agar colony formation assay, Chromatin immunoprecipitation (ChIP) assay and Luciferase promoter assay are described in the Supplementary Materials and methods.

3. Results

3.1. DGAT2 is upregulated in HFD-treated mice and metastatic GC patients

We first investigated whether HFD prompts peritoneal metastasis *in vivo*. The results shows that the peritoneal metastatic nodules of BGC823 and HGC27 GC cells were significantly increased in the HFD-fed mice compared with the control group mice (Fig. 1A and B). Moreover, HFD-fed mice had significantly shorter survival times than lean-fed controls (Fig. 1B). Notably, in pathological slices stained with H&E and Oil Red O, we found that the tumor cells adjacent to adipocytes displayed a more aggressive phenotype in HFD-fed SCID mice than in control diet mice (Fig. 1A). Monitoring of the mesenteric adipose tissue and body weights throughout the study showed that HFD significantly increased body weight and fat deposition in the mesentery of both nude mice (after 3 months) and SCID mice (after 2 months) (Figs. S1A–D). In nude mice, serum triglycerides and cholesterol (both LDL-c and HDL-c) were higher in the HFD group than in lean-fed mice (Fig. S1E).

To further explore the underlying mechanism of HFD-induced peritoneal metastasis, key enzymes involved in FA metabolism in the metastatic nodules of BGC823 cells were examined (Fig. 1C). It was reasonable to notice upregulation of the most prevalent FA transporter CD36, triglyceride synthase pathway proteins (GPD1/2, GPAT1, AGPAT1, PAP, DGAT1/2), fatty acid oxidation key enzyme CPT1A and NADPH-producing enzymes (NADK2, NNT) in the metastatic nodules of HFD-fed mice compared with the control (Fig. 1D). Intriguingly, DGAT2 was found to be the most significantly elevated among the enzymes detected (Fig. 1D), indicating DGAT2 may play critical roles in peritoneal metastasis after HFD.

More importantly, progressive overexpression of DGAT2 was observed in lymph node metastatic tissues compared with paired primary tumor analyzed using a tissue microarray (Fig. 1E and F). Also, DGAT2 expression level was significantly higher in tumor cells adjacent adipocytes than distant from adipocytes. (Fig. 1E and F). Although no significant difference of DGAT2 expression was observed between paired tumor and nontumorous tissues, there was notable increasement in paired metastasis and primary tumor tissues (Fig. 1F), which was further validated via immunoblotting analysis (Fig. 1G). Kaplan-Meier survival analysis showed that GC patients with high DGAT2 expression levels have a shorter overall survival and disease-free survival (Fig. 1H). Multivariate analysis also indicated that the DGAT2 expression was an independent prognostic factor in GC patients (Supplementary Table 2). In summary, these above results indicates that overexpression of DGAT2 was associated with increased GC omental metastasis in high fat conditions.

3.2. DGAT2 promotes adipocyte-induced LD formation and NADPH production

The omentum adipocytes were recently found to promote FA metabolism, LD formation and distant metastasis [19]. To clarify the precise molecular mechanism by which upregulated DGAT2 regulates these processes, purified adipocytes were obtained from human omental adipose tissues and verified with Oil Red O staining (Fig. 2A). Coculture of BGC823 and HGC27 cells with adipocytes (1:2) using 0.4-μm-pore transwell inserts resulted in stronger Oil Red O and BODIPY 493/503 staining intensity compared with that in the control group (Fig. 2A), indicating active formation of LDs. Moreover, the expression of DGAT2 was induced by coculture with adipocyte or treatment with oleic acid at both the mRNA and protein levels (Fig. 2B and C). To test whether DGAT2 was responsible for the formation of LDs in GC cells after coculture with adipocytes, DGAT2 was stably silenced in BGC823 and HGC27 cells (Fig. 2D). further study shows that DGAT2 knockdown significantly suppressed the uptake of fatty acids and the synthesis of TGs in GC cells (Fig. 2E and F), suggesting that DGAT2 mediates re-esterification of FAs in lipid-rich conditions.

Recent studies have provided solid evidence to support a “lipolytic phenotype” and an extensive dependence on FAO for the survival of cancer cells during oxidative stress and metastatic progression [21]. Gene set enrichment analyses revealed that the FA and glutathione metabolism pathways were significantly activated when DGAT2 was upregulated (Fig. 2G). Recent studies and our previous findings indicate that inhibition of FAO controls the NADPH level [9,11]. As shown in Fig. 2H, the enhanced GSH and NADPH production induced by coculture with adipocytes was completely blocked by knockdown of DGAT2 (Fig. 2H). Collectively, these data suggest that DGAT2 plays an important role in adipocyte-induced LD formation and NADPH production.

3.3. DGAT2 promotes cell anoikis resistance by redox modification

Anoikis resistance is critical for successful peritoneal colonization of GC [7]. When exposed to oxidative stress (H_2O_2, 150 μM, 48 h), GC cells experienced significant depletion of glutathione and NADPH (Fig. S2A), resulting in ROS accumulation and elevated apoptosis rates, which could be reversed by coculture with adipocytes (Fig. 3A). However, knockdown of DGAT2 significantly abolished the protective effects of adipocytes (Fig. 3A). Moreover, intracellular mitochondrial ROS (Mito-Sox) as well as total ROS (DCF-DA) were decreased in detached BGC823 and HGC27 cells cocultured with adipocytes, and these effects were blocked by DGAT2 knockdown (Fig. 3B). Calcein AM/EthD-1 staining was applied to label live cells with green fluorescence and cells undergoing anoikis with red fluorescence. Coculture with adipocytes or treatment with oleic acid decreased the red/green fluorescence ratio of GC cells, while knockdown of DGAT2 increased anoikis under detached conditions (Figs. 3C, 3D, S2B and S2C). Most importantly, the proapoptotic effects of DGAT2 inhibition were completely reversed by pretreatment with the antioxidant NAC (2 mM) (Fig. 3E and F). These results indicate that depletion of DGAT2 enhances anoikis through ROS-mediated mechanisms.

3.4. DGAT2 promotes HFD-induced peritoneal dissemination and lung metastasis in vivo

To determine the effects of DGAT2 *in vivo*, knockdown and control cells were injected into the peritoneal cavities of mice. The results showed that DGAT2 suppression significantly reduced mesenteric metastatic nodules in the intestinal wall of the HFD nude mice and the SCID mice (Fig. 4A–D). These findings support the idea that obesity facilitates GC peritoneal dissemination via upregulation of DGAT2.

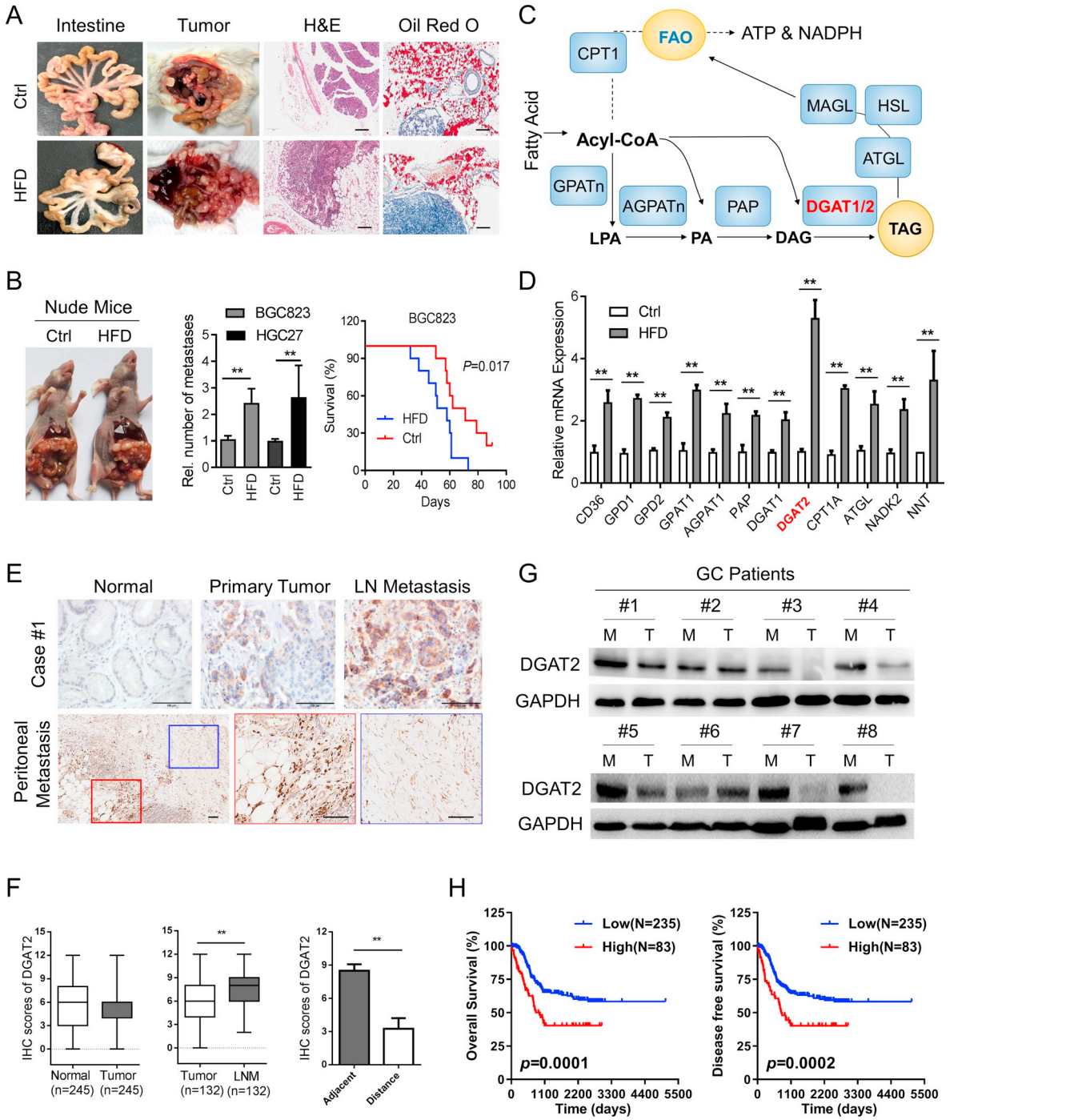

Fig. 1. DGAT2 is upregulated in HFD-treated mice and GC patients with metastasis. **(A)** Representative images of adipose tissue in intestine and mesentery of SCID mice fed with control diet or HFD for 60 days. The BGC823 cells metastases in the colonic wall was recorded. H&E and Oil Red O staining of peritoneal nodule was performed (scale bar = 200 μm). **(B)** Representative images and quantification of metastases in nude mice injected with gastric cancer cells. Influence of the HFD on tumor-bearing mice survival times were measured with Kaplan-Meier survival curves (N = 10 mice per group). **(C)** Graphical description of the relationship between DGAT and fatty acid metabolism. **(D)** qPCR analysis of the indicated gene expression involved in lipid metabolism of the peritoneal metastatic nodules of BGC823 cells in SCID mice. **(E)** Representative immunohistochemical (IHC) staining in human primary GC tumor tissues and paired lymph node metastasis tissues (scale bar = 100 μm). Representative IHC staining in human GC peritoneal metastases shows higher DGAT2 level in tumor cells adjacent adipocytes than distant. **(F)** The IHC staining scores of DGAT2 in paired primary GC tumor tissues (N = 245), or lymph node metastatic tissues (LN, N = 132). **(G)** Immunoblotting analysis of DGAT2 protein levels in 8 paired fresh metastasis and primary tumor tissues. **(H)** Kaplan–Meier analysis of overall survival or disease-free survival curves for GC patients with low versus high expression of DGAT2 (log-rank test). $^{**}P < 0.01$, Student's *t*-test, mean ± SD. (For interpretation of the references to colour in this figure legend, the reader is referred to the Web version of this article.)

Additionally, BGC823 and HGC27 cells were injected into the tail vein of nude mice, and then histologic examination was used to detect lung metastasis. H&E staining showed significantly more metastatic nodules in the HFD-fed group than in the control group (Fig. 4E and F). However, knockdown of DGAT2 markedly suppressed the lung metastasis of mice injected with BGC823 and HGC27 cells when fed with HFD (Fig. 4E and F). In summary, DGAT2 appears to be responsible for HFD-induced peritoneal dissemination and lung metastasis *in vivo*.

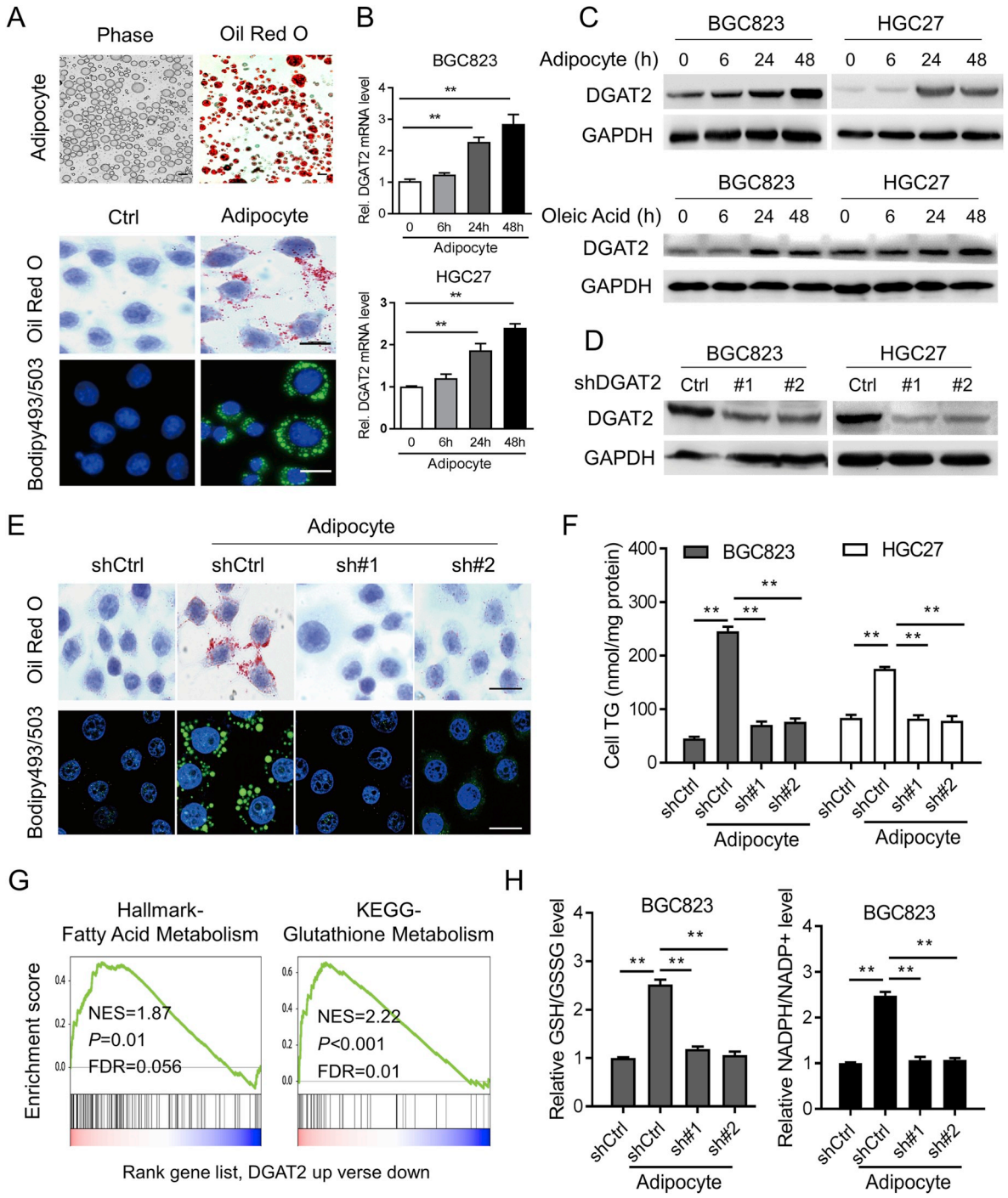

Fig. 2. DGAT2 promotes adipocyte-induced LD formation and NADPH production. **(A)** Phase-contrast micrograph and Oil Red O staining of adipocytes isolated from cancer-associated adipose tissues (Scale bars = 100 μm). Representative images of lipid droplets in BGC823 cells were detected using Oil Red O staining and BODIPY 493/503 staining (green), cell nuclei were stained with DAPI (blue) (Scale bars = 10 μm). **(B)** qPCR analysis of DGAT2 mRNA expression in indicated GC cells cultured with adipocyte for different times. **(C–D)** Immunoblotting analysis of DGAT2 levels in indicated GC cells, GAPDH was used as a loading control. **(E)** Oil Red O staining and confocal microscopy to detect lipid droplets by BODIPY 493/503 in scramble control and DGAT2 knockdown BGC823 cells (Scale bars = 10 μm). **(F)** Intracellular triglyceride (TG) accumulation was measured by triglyceride determination kit. **(G)** Gene set enrichment analyses identified the correlation of the FAs and glutathione metabolism pathway with DGAT2. **(H)** Measurement of NADPH/NADP + and GSH/GSSG levels in the indicated BGC823 cells cultured alone or with human adipocytes. $^{**}P < 0.01$, Student's *t*-test, mean ± SD. (For interpretation of the references to colour in this figure legend, the reader is referred to the Web version of this article.)

3.5. C/EBPα transcriptionally upregulates DGAT2 expression in gastric cancer

By mining the online database, less than 2.5% of GC samples presented with amplification or deletion of DGAT2 (Fig. 5A), which prompted us to investigate the transcription factors responsible for DGAT2 upregulation. Several candidates were screened out using the JASPAR database, and C/EBPα was selected due to its critical roles in adipogenesis, adipocyte development and lipid accumulation [31]. First, C/EBPα expression was positively correlated with DGAT2

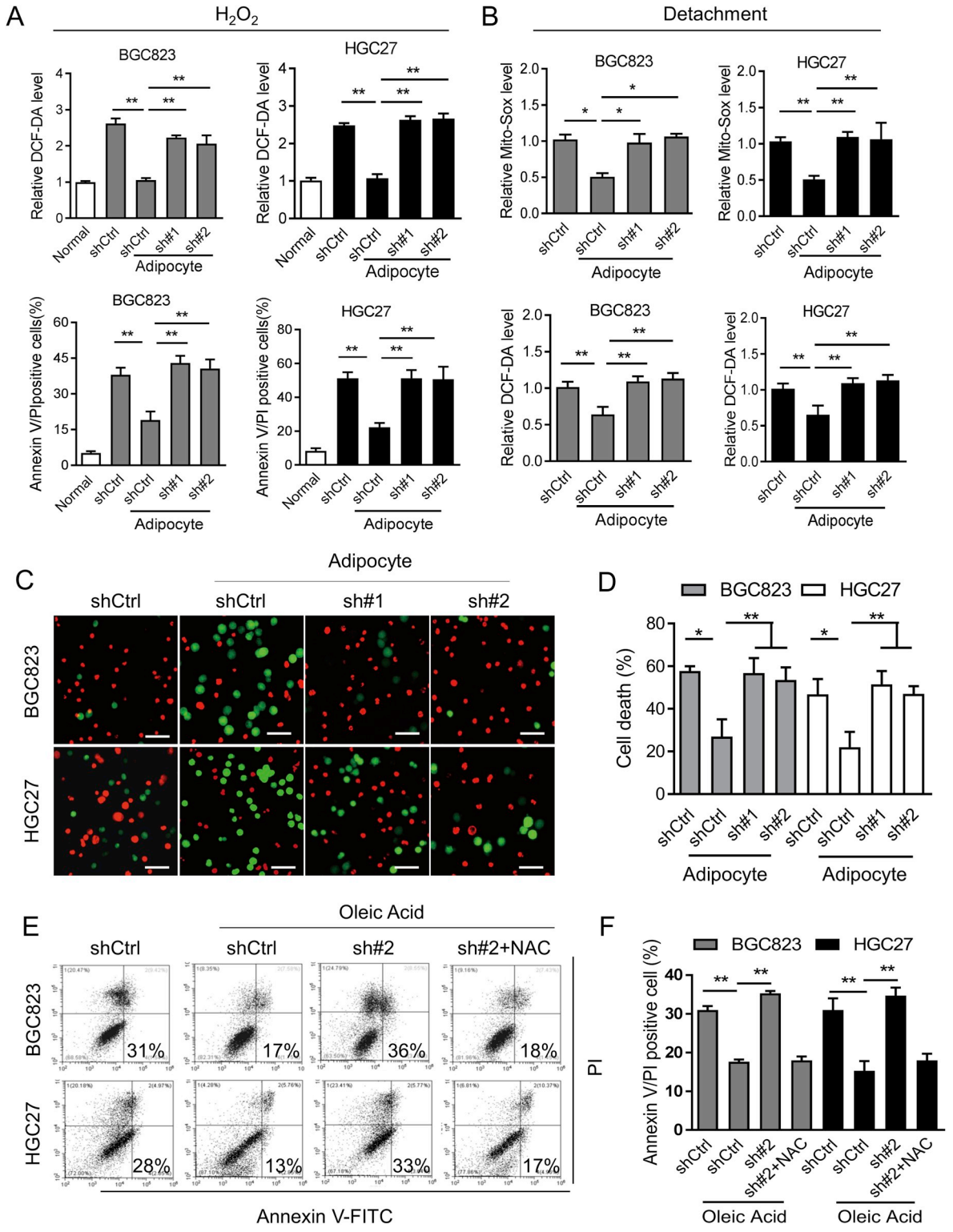

Fig. 3. DGAT2 promotes cell anoikis resistance by redox modification. **(A)** Flow analysis of intracellular ROS levels (detected by the fluorescent probe DCF-DA) and cell apoptosis (measured by Annexin-V/PI assay) in the indicated cells treated with H_2O_2 (150 μM) for 48 h. **(B)** Flow analysis of mitochondrial ROS and intracellular ROS levels in indicated GC cells under detachment. **(C–D)** Representative images and quantification of anoikis of indicated cells cultured alone or with adipocytes following withdrawal of extracellular matrix support for 48 hh (Scale bars = 50 μm). Calcein AM (green fluorescent dye) was used to detect cell viability and EthD-1 (red fluorescent dye) for cell death. **(E–F)** Representative images and quantification of cell apoptosis in DGAT2-knockdown and control cells treated with oleic acid (200 μM) following withdrawal of extracellular matrix support for 48 h. The antioxidant NAC (2 mM) was used. $^{**}P < 0.01$, Student's *t*-test, mean ± SD. (For interpretation of the references to colour in this figure legend, the reader is referred to the Web version of this article.)

expression at the mRNA level as analyzed in the TCGA dataset, Cancer Cell Line Encyclopedia (CCLE) and collected clinical GC samples in our institute, indicating transcriptional regulation of DGAT2 by C/EBPα (Fig. 5B and C). Second, knockdown of C/EBPα in BGC823 and HGC27 cells by siRNAs reduced both mRNA and protein levels of DGAT2, even in the presence of exogenous oleic acid (Fig. 5D–F). Third,

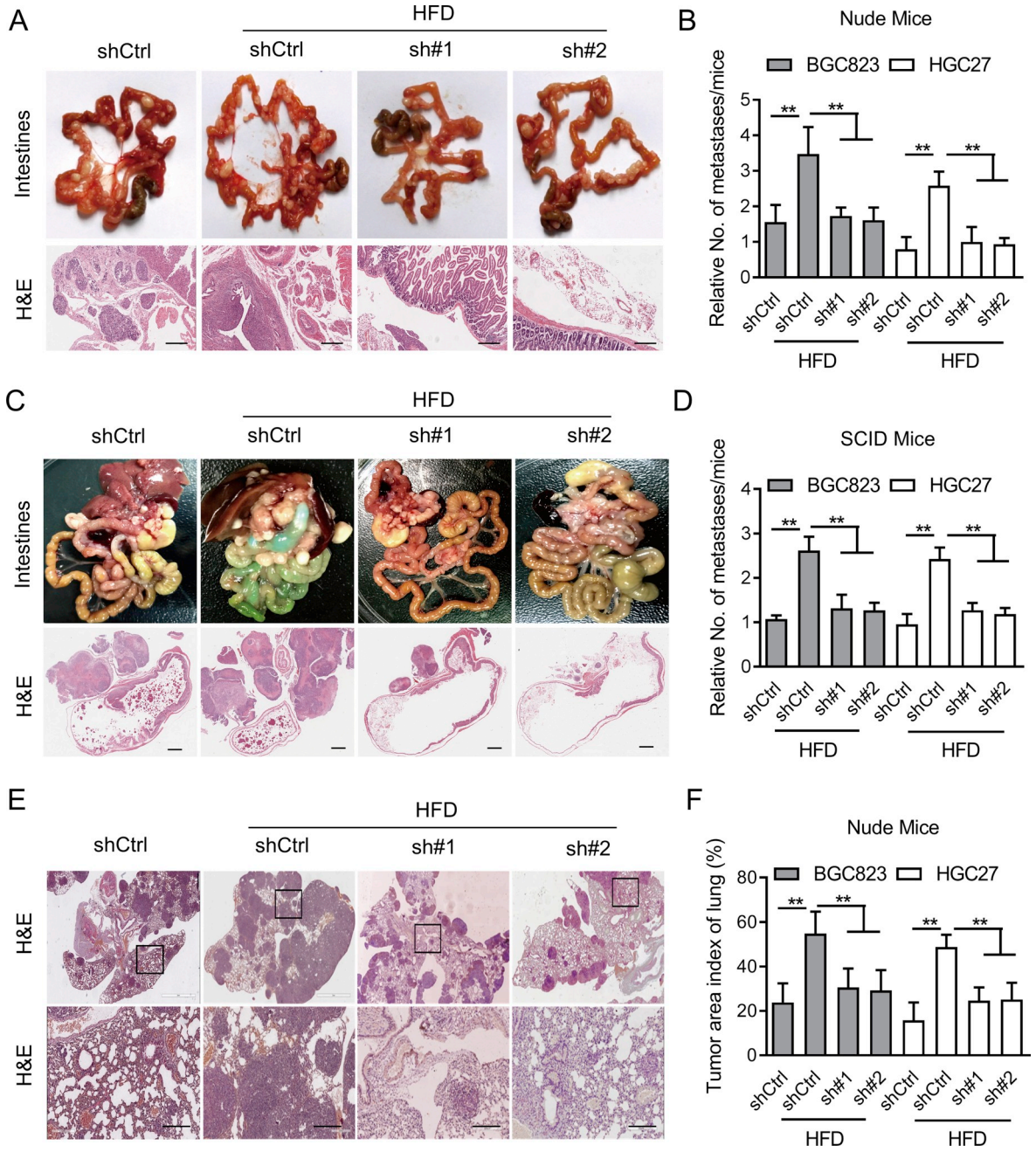

Fig. 4. DGAT2 promotes HFD-induced peritoneal dissemination and lung metastasis *in vivo*. Female nude or SCID mice fed the ctrl diet or HFD were injected intraperitoneally with 3×10^6 scrambled vector or DGAT2 shRNA transduced cells and were sacrificed after 30 days. **(A)** Representative intestines and H&E staining of scattered tumors in nude mice (N = 6). **(B)** The quantification of metastases in nude mice was counted. **(C–D)** Representative intestines and H&E staining of scattered tumors in SCID mice (N = 6). The quantification of metastases in SCID mice was counted. **(E)** Representative results of H&E staining of metastatic lung nodules from nude mice injected with DGAT2 knockdown and control cells via the tail vein for 30 days (scale bars = 200 μm). **(F)** Metastatic nodules under the microscope were counted and recorded. $^{**}P < 0.01$, Student's *t*-test, mean ± SD.

two C/EBPα response elements were found in the DGAT2 promoter (Fig. 5G). ChIP-qPCR assays further demonstrated that C/EBPα could bind to the promotor of DGAT2 (Fig. 5H), while knockdown of C/EBPα significantly decreased the luciferase activity of the DGAT2 promoter in BGC823 and HGC27 cells (Fig. 5I). Fourth, IHC analysis of GC tissue specimens showed a significant positive correlation between C/EBPα and DGAT2 (Fig. 5J). Altogether, these results demonstrate that DGAT2 was transcriptionally upregulated by C/EBPα in gastric cancer.

3.6. PF-06424439 suppresses gastric cancer metastasis in vitro and in vivo

PF-06424439 was an orally bioavailable small-molecule DGAT2 inhibitor evaluated *in vivo* [32]. We therefore tested its antitumor activity in GC and found that PF-06424439 treatment for 12 h almost completely blocked the formation of LDs in BGC823 and HGC27 cells cocultured with adipocytes or treatment with oleic acid (Fig. 6A). Moreover, the antiapoptotic effects of adipocytes when exposed to detached conditions or H_2O_2 were blocked by the DGAT2 inhibitor PF-06424439, as indicated by calcein AM/EthD-1 staining and flow analysis (Fig. 6B). To determine the effects of the DGAT2 inhibitor PF-

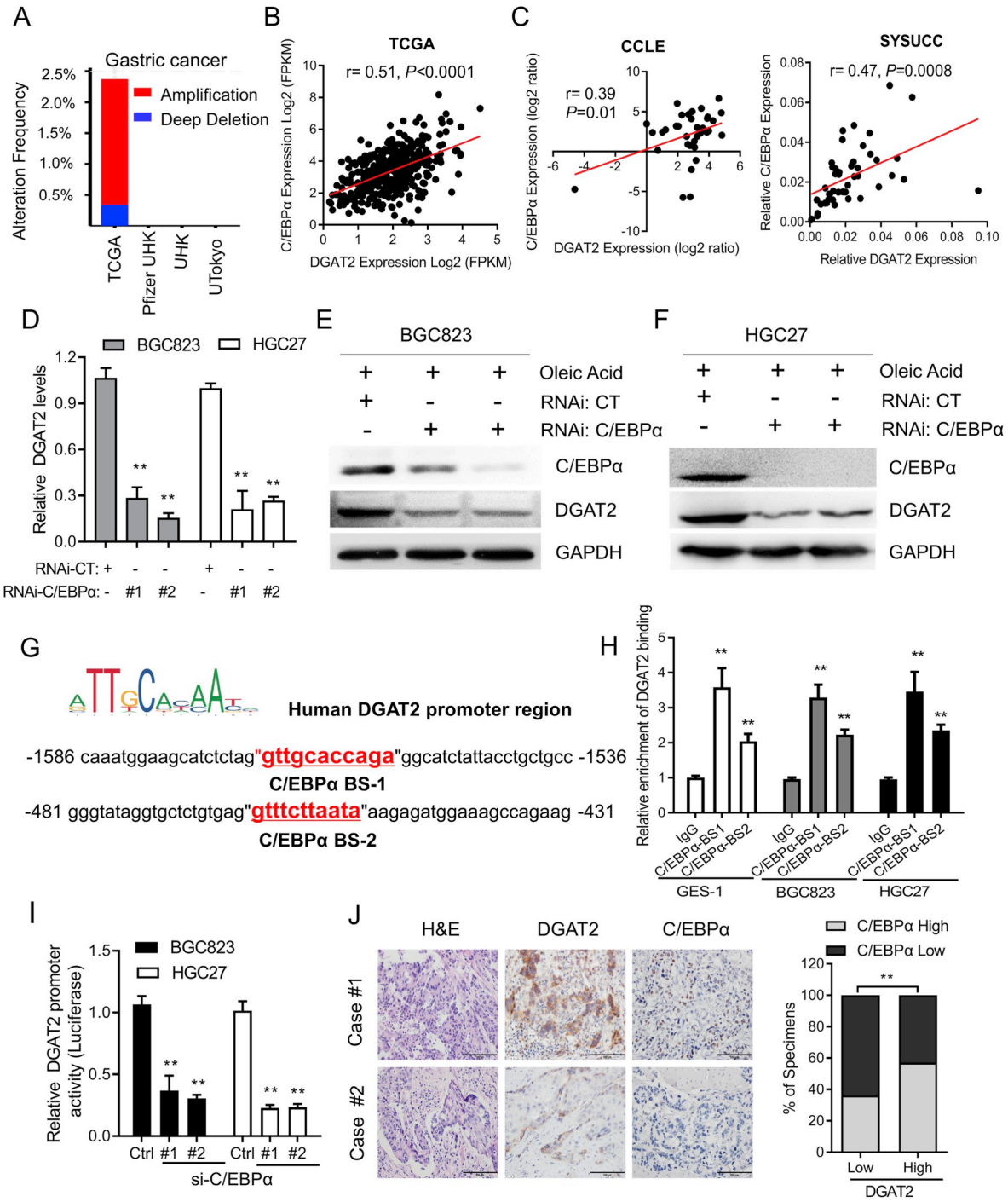

Fig. 5. C/EBPα upregulates DGAT2 expression in GC. (A) Distribution of alteration frequency of DGAT2 in the TCGA gastric cancer dataset. **(B)** Scatterplots of DGAT2 vs C/EBPα mRNA expression in the TCGA dataset analyzed by qPCR. **(C)** Scatterplots of DGAT2 vs C/EBPα mRNA expression in gastric cell lines available from CCLE database (N = 37) and our collected clinical gastric cancer samples (N = 47). Pearson correlation coefficient (r) and *P* value are displayed. **(D)** qPCR analysis of DGAT2 expression in BGC823 and HGC27 cells after siRNA-mediated knockdown of C/EBPα cultured with 200 μM oleic acid. **(E–F)** Immunoblotting analysis of DGAT2 expression in BGC823 and HGC27 cells after siRNA-mediated knockdown of C/EBPα. **(G)** C/EBPα DNA-binding sites are present in the human DGAT2 promoter region. **(H)** Enrichment of C/EBPα binding of DGAT2 promoter at indicated GC cell line. **(I)** Relative DGAT2 luciferase promoter activity in BGC823 and HGC27 cells with C/EBPα depletion. **(J)** Representative image and correlations analysis of DGAT2 and C/EBPα expression in gastric cancer tissues (scale bar = 100 μm). Chi-square test was used to study the association between DGAT2 and C/EBPα expression. $^{**}P < 0.01$, Student's *t*-test, mean ± SD.

06424439 on GC peritoneal metastasis *in vivo*, BGC823 and HGC27 cells were injected into the peritoneal cavities of SCID mice and nude mice. The results indicated that PF-06424439 significantly reduced mesenteric metastasis (Fig. 6C and D). These findings indicate that PF-06424439 displays therapeutic activity against gastric cancer, which merits further clinical investigation.

4. Discussion

GC patients diagnosed with omental metastasis, irrespective of T- or N-stage, number of metastases, or anatomical location of primary cancer, present with poor prognosis and have limited therapy options [33]. Body mass index was identified as an independent prognostic

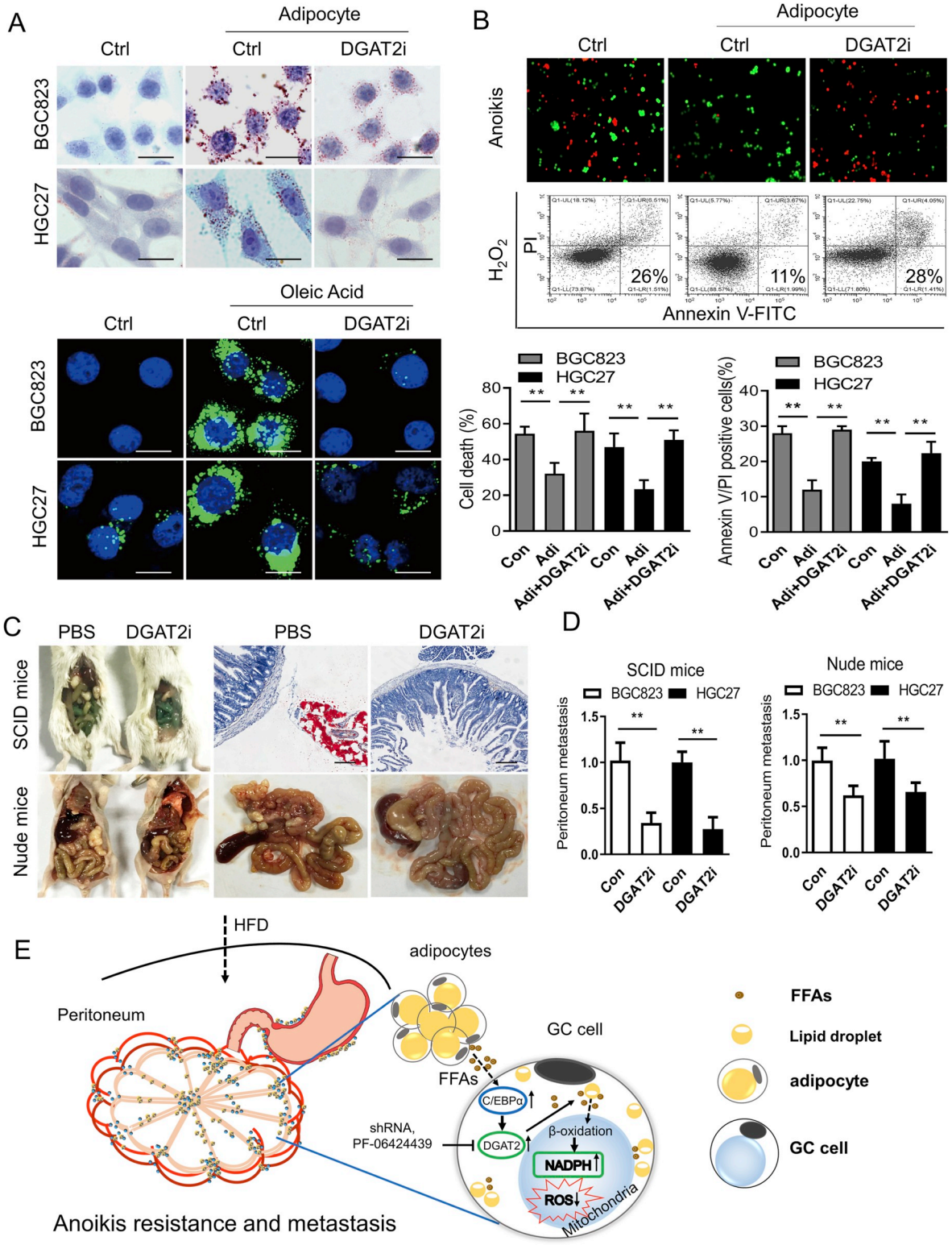

Fig. 6. The DGAT2 inhibitor PF-06424439 suppresses metastasis of GC *in vitro* and *in vivo*. (A) Representative lipid droplets in indicated GC cells following coculture with adipocyte or treatment with oleic acid (200 μM), as detected by Oil Red O staining (Scale bars = 10 μm). DGAT2 inhibitor PF-06424439 (20 μM) was used. **(B)** Representative apoptotic cells were visualized by calcein AM/EthD-1 or by Annexin-V/PI assay in indicated cells treated with anoikis or H_2O_2 (150 μM) for 48 h, respectively. Quantification data are shown at down panel. **(C–D)** Representative images and statistical results of scattered tumors in the intestines of mice (N = 5) (Scale bars = 100 μm). **(E)** Proposed working model of this study. $^{**}P < 0.01$, Student's *t*-test, mean ± SD. (For interpretation of the references to colour in this figure legend, the reader is referred to the Web version of this article.)

factor for GC with peritoneal seeding. Additionally, omental metastatic cancer cells might be largely dependent on the local microenvironment to survive. Despite a long recognition that omental tissue is composed of adipocytes and plays a more central role in the secretion of pro-cancerous cytokines than subcutaneous adipose tissue [34], relatively little attention has been paid to the mechanistic interaction between

gastric cancer cells and adipocytes.

Previous studies have uncovered critical roles of inflammation, adipose stromal cells, adipokines and hormones behind crosstalk between adipocytes and cancer [34]. Obesity-associated hepatic oxidative stress activates STAT3 signaling via dephosphorylation, resulting in pathogenesis of hepatocellular carcinoma [35], while selective knockout of p62 in adipocytes promotes metastatic aggressiveness of prostate carcinoma *in vivo* through upregulation of osteopontin secretion, which is vital for the oxidation of FAs and the invasion of cancer cells [36]. More recently, it was found that adipocyte-derived FAs can be oxidized by cancer cells and ultimately utilized to fuel peritoneal metastasis [17,19,37], which is in accordance with our findings that omental adipocytes might provide a niche as a fatty acid reservoir to support GC cell colonization.

Cancer cells often require much more NADPH supplementation for redox hemostasis, which is critical for cancer cell survival under energy stress conditions, such as anchorage-independent growth, than their normal counterparts [6,7,38–40]. To overcome ROS stress and metastasize to the peritoneum, cancer cells may develop anoikis resistance through several mechanisms, including metabolic reprogramming [41]. FAO is an important source of NADPH, as the end-product acetyl CoA can enter the Krebs cycle, giving rise to citrate, which is then exported to the cytoplasm and produces cytosolic NADPH through metabolic chain reactions(9), and the ultimate hydrogen acceptor NADH can be converted to NADPH through the nicotinamide nucleotide transhydrogenase pathway [42]. The production of FAO-derived cytosolic NADPH is key for cancer cells to overcome oxidative stress [10,43]. However, exogenous FAs need to be transformed into TGs to avoid lipid toxicity and stored as LDs before oxidation to supply NADPH.

DGAT2 is the key enzyme by which cells metabolize exogenous FAs to form TGs. However, less is known about its roles in cancer progression, especially during the peritoneal metastasis of GC. Herein, we utilized a HFD *in vivo* mouse model and human patient-derived tissues to determine how adipocytes promote GC progression. In this study, we demonstrated that DGAT2 is upregulated in GC, and its expression is closely related to patient survival. Furthermore, DGAT2 expression is increased by fatty acids, and C/EBPα binds to the DGAT2 gene promoter to upregulate DGAT2 transcriptionally.

In summary, our study demonstrated that adipocytes can donate FAs to GC cells, fueling NADPH synthesis and anoikis resistance. These adipocyte-derived FAs are transported into GC cells to form lipid droplets, after which DGAT2 is induced to catalyze re-esterification of FAs from adipocytes. Upregulation of DGAT2 increases the rate of intracellular lipid metabolism and provides NADPH for ROS elimination during peritoneal metastasis. More importantly, pharmacological inhibition of DGAT2 leads to significant inhibition of peritoneal metastasis of GC *in vivo* (Fig. 6E). Our study highlights the notion that DGAT2 may be a promising therapeutic target in GC with peritoneal implantation and provides some evidence for uncovering the link between obesity and tumor metastasis.

5. Conclusions

Our findings highlight the crucial functional roles of DGAT2 in tumor metastasis and tumor progression in gastric cancer. Understanding DGAT2-dependent lipid droplets accumulation and redox homeostasis may be a promising therapeutic target in GC with peritoneal implantation and provide some evidence for uncovering the link between obesity and tumor metastasis. Inhibition of DGAT2 may be a promising therapeutic alternative in gastric cancer treatment.

Funding

This work was supported by the Natural Science Foundation of China (81702886), the Natural Science Foundation of Guangdong Province (2017A030310552, 2019A1515010233), the Science Technology and Innovation Foundation of Guangzhou (201607010046), the Education Department of Guangdong Province (2019KZDXM058, 2016KQNCX139).

Authors' contributions

S. Li and T. Tian designed the study. S. Li, T. Wu, Y.-X. Lu, J.-X. Wang, F.-H. Yu, M.-Z. Yang, Y.-J. Huang, Z.-J. Li, S.-L. Wang, L. Huang and L. Lu performed the *in vitro* and animal experiments. S. Li, T. Wu, Y.-X. Lu and T. Tian analyzed the data. S. Li, T. Wu and Y.-X. Lu wrote the manuscript. All authors read and approved the final manuscript.

Declaration of competing interest

The authors declare no conflicts.

Acknowledgements

The authors thank Prof. Huai-Qiang Ju (Sun Yat-sen University Cancer Center) for helpful discussion and constructive suggestions.

Appendix A. Supplementary data

Supplementary data to this article can be found online at https://doi.org/10.1016/j.redox.2020.101596.

References

[1] J. Ferlay, H.R. Shin, F. Bray, D. Forman, C. Mathers, D.M. Parkin, Estimates of worldwide burden of cancer in 2008: globocan 2008, Int. J. Canc. 127 (12) (2010) 2893–2917.
[2] E.E. Calle, R. Kaaks, Overweight, obesity and cancer: epidemiological evidence and proposed mechanisms, Nat. Rev. Canc. 4 (8) (2004) 579–591.
[3] C. Ga, L.L. Peterson, Obesity and cancer: evidence, impact, and future directions, Clin. Chem. 64 (1) (2018) 154–162.
[4] K.I. Avgerinos, N. Spyrou, C.S. Mantzoros, M. Dalamaga, Obesity and cancer risk: emerging biological mechanisms and perspectives, Metabolism 92 (2019) 121–135.
[5] I. Thomassen, Y.R. van Gestel, B. van Ramshorst, M.D. Luyer, K. Bosscha, S.W. Nienhuijs, et al., Peritoneal carcinomatosis of gastric origin: a population-based study on incidence, survival and risk factors, Int. J. Canc. 134 (3) (2014) 622–628.
[6] S. Li, Z. Zhuang, T. Wu, J.C. Lin, Z.X. Liu, L.F. Zhou, et al., Nicotinamide nucleotide transhydrogenase-mediated redox homeostasis promotes tumor growth and metastasis in gastric cancer, Redox Biol 18 (2018) 246–255.
[7] Y.X. Lu, H.Q. Ju, Z.X. Liu, D.L. Chen, Y. Wang, Q. Zhao, et al., ME1 regulates NADPH homeostasis to promote gastric cancer growth and metastasis, Canc. Res. 78 (8) (2018) 1972–1985.
[8] Y. Wang, J.H. Lu, F. Wang, Y.N. Wang, M.M. He, Q.N. Wu, et al., Inhibition of fatty acid catabolism augments the efficacy of oxaliplatin-based chemotherapy in gastrointestinal cancers, Canc. Lett. 473 (2020) 74–89.
[9] A. Carracedo, L.C. Cantley, P.P. Pandolfi, Cancer metabolism: fatty acid oxidation in the limelight, Nat. Rev. Canc. 13 (4) (2013) 227–232.
[10] S.M. Jeon, N.S. Chandel, N. Hay, AMPK regulates NADPH homeostasis to promote tumour cell survival during energy stress, Nature 485 (7400) (2012) 661–665.
[11] Y.N. Wang, Z.L. Zeng, J. Lu, Y. Wang, Z.X. Liu, M.M. He, et al., CPT1A-mediated fatty acid oxidation promotes colorectal cancer cell metastasis by inhibiting anoikis, Oncogene 37 (46) (2018) 6025–6040.
[12] E.M. Griner, M.G. Kazanietz, Protein kinase C and other diacylglycerol effectors in cancer, Nat. Rev. Canc. 7 (4) (2007) 281–294.
[13] G. Pascual, A. Avgustinova, S. Mejetta, M. Martin, A. Castellanos, C.S. Attolini, et al., Targeting metastasis-initiating cells through the fatty acid receptor CD36, Nature 541 (7635) (2017) 41–45.
[14] A.J. Hoy, S. Balaban, D.N. Saunders, Adipocyte-tumor cell metabolic crosstalk in breast cancer, Trends Mol. Med. 23 (5) (2017) 381–392.
[15] C. Zhang, C. Yue, A. Herrmann, J. Song, C. Egelston, T. Wang, et al., STAT3 activation-induced fatty acid oxidation in CD8(+) T effector cells is critical for obesity-promoted breast tumor growth, Cell Metabol. 31 (1) (2020) 148–161 e5.
[16] F. Miranda, D. Mannion, S. Liu, Y. Zheng, L.S. Mangala, C. Redondo, et al., Salt-inducible kinase 2 couples ovarian cancer cell metabolism with survival at the adipocyte-rich metastatic niche, Canc. Cell 30 (2) (2016) 273–289.
[17] K.M. Nieman, H.A. Kenny, C.V. Penicka, A. Ladanyi, R. Buell-Gutbrod, M.R. Zillhardt, et al., Adipocytes promote ovarian cancer metastasis and provide energy for rapid tumor growth, Nat. Med. 17 (11) (2011) 1498–1503.
[18] I. Lazar, E. Clement, S. Dauvillier, D. Milhas, M. Ducoux-Petit, S. LeGonidec, et al., Adipocyte exosomes promote melanoma aggressiveness through fatty acid oxidation: a novel mechanism linking obesity and cancer, Canc. Res. 76 (14) (2016) 4051–4057.

[19] Y. Tan, K. Lin, Y. Zhao, Q. Wu, D. Chen, J. Wang, et al., Adipocytes fuel gastric cancer omental metastasis via PITPNC1-mediated fatty acid metabolic reprogramming, Theranostics 8 (19) (2018) 5452–5468.
[20] C.L. Yen, S.J. Stone, S. Koliwad, C. Harris, R.V. Farese Jr., Thematic review series: glycerolipids. DGAT enzymes and triacylglycerol biosynthesis, J. Lipid Res. 49 (11) (2008) 2283–2301.
[21] Q. Liu, R.M. Siloto, R. Lehner, S.J. Stone, R.J. Weselake, Acyl-CoA:diacylglycerol acyltransferase: molecular biology, biochemistry and biotechnology, Prog. Lipid Res. 51 (4) (2012) 350–377.
[22] F. Wilfling, H. Wang, J.T. Haas, N. Krahmer, T.J. Gould, A. Uchida, et al., Triacylglycerol synthesis enzymes mediate lipid droplet growth by relocalizing from the ER to lipid droplets, Dev. Cell 24 (4) (2013) 384–399.
[23] S.J. Stone, M.C. Levin, P. Zhou, J. Han, T.C. Walther, R.V. Farese Jr., The endoplasmic reticulum enzyme DGAT2 is found in mitochondria-associated membranes and has a mitochondrial targeting signal that promotes its association with mitochondria, J. Biol. Chem. 284 (8) (2009) 5352–5361.
[24] S. Cases, S.J. Smith, Y.W. Zheng, H.M. Myers, S.R. Lear, E. Sande, et al., Identification of a gene encoding an acyl CoA:diacylglycerol acyltransferase, a key enzyme in triacylglycerol synthesis, Proc. Natl. Acad. Sci. U. S. A. 95 (22) (1998) 13018–13023.
[25] S. Cases, S.J. Stone, P. Zhou, E. Yen, B. Tow, K.D. Lardizabal, et al., Cloning of DGAT2, a second mammalian diacylglycerol acyltransferase, and related family members, J. Biol. Chem. 276 (42) (2001) 38870–38876.
[26] S.J. Stone, H.M. Myers, S.M. Watkins, B.E. Brown, K.R. Feingold, P.M. Elias, et al., Lipopenia and skin barrier abnormalities in DGAT2-deficient mice, J. Biol. Chem. 279 (12) (2004) 11767–11776.
[27] H.Q. Ju, Y.X. Lu, Q.N. Wu, J. Liu, Z.L. Zeng, H.Y. Mo, et al., Disrupting G6PD-mediated Redox homeostasis enhances chemosensitivity in colorectal cancer, Oncogene 36 (45) (2017) 6282–6292.
[28] W. Li, C.P. Yu, J.T. Xia, L. Zhang, G.X. Weng, H.Q. Zheng, et al., Sphingosine kinase 1 is associated with gastric cancer progression and poor survival of patients, Clin. Canc. Res. 15 (4) (2009) 1393–1399.
[29] J. Hq, L. Yx, C. Dl, Z. Zx, L. Zx, W. Qn, et al., Modulation of redox homeostasis by inhibition of MTHFD2 in colorectal cancer: mechanisms and therapeutic implications, J. Natl. Cancer Inst. 111 (6) (2019) 584–596.
[30] H.Q. Ju, H. Ying, T. Tian, J. Ling, J. Fu, Y. Lu, et al., Mutant Kras- and p16-regulated NOX4 activation overcomes metabolic checkpoints in development of pancreatic ductal adenocarcinoma, Nat. Commun. 8 (2017) 14437.
[31] J.E. Lee, H. Schmidt, B. Lai, K. Ge, Transcriptional and epigenomic regulation of adipogenesis, Mol. Cell Biol. 39 (11) (2019).
[32] K. Futatsugi, D.W. Kung, S.T. Orr, S. Cabral, D. Hepworth, G. Aspnes, et al., Discovery and optimization of imidazopyridine-based inhibitors of diacylglycerol acyltransferase 2 (DGAT2), J. Med. Chem. 58 (18) (2015) 7173–7185.
[33] N. Bernards, G.J. Creemers, G.A. Nieuwenhuijzen, K. Bosscha, J.F. Pruijt, V.E. Lemmens, No improvement in median survival for patients with metastatic gastric cancer despite increased use of chemotherapy, Ann. Oncol. 24 (12) (2013) 3056–3060.
[34] C. Himbert, M. Delphan, D. Scherer, L.W. Bowers, S. Hursting, C.M. Ulrich, Signals from the adipose microenvironment and the obesity-cancer link-A systematic review, Canc. Prev. Res. 10 (9) (2017) 494–506.
[35] M. Grohmann, F. Wiede, G.T. Dodd, E.N. Gurzov, G.J. Ooi, T. Butt, et al., Obesity drives STAT-1-dependent NASH and STAT-3-dependent HCC, Cell 175 (5) (2018) 1289–1306 e20.
[36] J. Huang, A. Duran, M. Reina-Campos, T. Valencia, E.A. Castilla, T.D. Muller, et al., Adipocyte p62/SQSTM1 suppresses tumorigenesis through opposite regulations of metabolism in adipose tissue and tumor, Canc. Cell 33 (4) (2018) 770–784 e6.
[37] A. Ladanyi, A. Mukherjee, H.A. Kenny, A. Johnson, A.K. Mitra, S. Sundaresan, et al., Adipocyte-induced CD36 expression drives ovarian cancer progression and metastasis, Oncogene 37 (17) (2018) 2285–2301.
[38] C.A. Lewis, S.J. Parker, B.P. Fiske, D. McCloskey, D.Y. Gui, C.R. Green, et al., Tracing compartmentalized NADPH metabolism in the cytosol and mitochondria of mammalian cells, Mol. Cell. 55 (2) (2014) 253–263.
[39] N.N. Pavlova, C.B. Thompson, The emerging hallmarks of cancer metabolism, Cell Metabol. 23 (1) (2016) 27–47.
[40] H.Q. Ju, Y.X. Lu, D.L. Chen, Z.X. Zuo, Z.X. Liu, Q.N. Wu, et al., Modulation of redox homeostasis by inhibition of MTHFD2 in colorectal cancer: mechanisms and therapeutic implications, J. Natl. Cancer Inst. 111 (6) (2019) 584–596.
[41] J.A. Mason, K.R. Hagel, M.A. Hawk, Z.T. Schafer, Metabolism during ECM detachment: achilles heel of cancer cells? Trends Cancer 3 (7) (2017) 475–481.
[42] M.P. Murphy, Redox modulation by reversal of the mitochondrial nicotinamide nucleotide transhydrogenase, Cell Metabol. 22 (3) (2015) 363–365.
[43] I. Samudio, R. Harmancey, M. Fiegl, H. Kantarjian, M. Konopleva, B. Korchin, et al., Pharmacologic inhibition of fatty acid oxidation sensitizes human leukemia cells to apoptosis induction, J. Clin. Invest. 120 (1) (2010) 142–156.